A Radio System for Detecting Pulses from Cosmic Ray Extensive Air Showers

NAZZARENO MANDOLESI GIORGIO G.C. PALUMBO

Laboratorio Studio e Tecnologie delle Radiazioni Extraterrestri.

C.N.R.

ISTITUTO DI FISICA - UNIVERSITA' DI BOLOGNA

GIANFRANCO SINIGAGLIA GOLIARDO TOMASSETTI

Laboratorio Nazionale di Radioastronomia

ISTITUTO DI FISICA - UNIVERSITA' DI BOLOGNA.

Abstract

A radio receiving system for detection of radio pulses from Extensive Air Showers has been built.
Such system was formed of two radio channels simultaneously triggered by a three scintillators shower array. The first channel was fed by an array of four Yagi 30 MHz antennae. The second channel was fed by an 11 elements Yagi antenna at 408 MHz. Both receiving systems are described and their sensitivity discussed as well as noise temperature.

Riassunto

Si è costruito un sistema per rivelare radio impulsi da Sciami Estesi.
Tale sistema è formato da due radio ricevitori simultaneamente interrogati dalla coincidenza di 3 scintillatori costituenti un rivelatore di sciami. Al primo radio ricevitore viene inviata l'uscita di un gruppo di 4 antenne a 30 MHz mentre al secondo l'uscita di una antenna a 408 MHz a 11 elementi. Vengono descritti entrambi i sistemi riceventi e viene discussa la temperatura del rumore insieme alla loro sensibilità.

Introduction

A coherent emission from Extensive Air Showers (EAS) at meter wavelengths was foreseen by Askaryan [1] since 1961. A calculated 8% negative excess in the shower disc was the supposed cause of the emission. Jelley et al.[2] in 1965 for the first time detected radio pulses from EAS at 44 MHz. Since then several hypotheses have been made and much experimental work has been done in order to better understand the phenomenon.

However, many problems are still unsolved. Most likely, coherent radiation is produced by charge separation in the Earth's magnetic field, as suggested by Kahn and Lerche [3] . Only a small contribution to the emission seems to be given by charge excess [4] as shown also by polarization measurements [5] . The frequency range according to coherence conditions goes from a few MHz to ~ 75 MHz. While the frequency spectrum has been explored before up to 60 MHz [6,7] very little information is available at higher frequencies. The possibility of detecting pulses at short wavelengths was forwarded by Filchenkov and Rosenthal [8] . Such radiation should be incoherent, according to the authors, and detectable over a much larger area than the coherent one. The incoherent radiation predicted should be due to bremsstrahlung but a recent discussion by Charman and Jelley [9] suggests that is is unlikely to be important under normal conditions. A Dublin group [10] and more recently Spencer [11] and Charman and Jelley [12] have done exploratory work in the U.H.F. region.

Results seem to suggest incoherent emission; however, a coherent effect is not contradictory with the data.

Investigation in the short wavelength region is tempting since both man-made interference and sky temperature are lower than in the meter wavelengths region. Furthermore the presence of radio emission at high frequencies could notably change the shape of the frequency spectrum predicted by coherent theories [1,3,13] and increase the possibility of detecting EAS by solely radio techniques.

An experiment has been performed by our Group in order to check emission at 30 MHz, and to gather further information about coherent radiation. Simultaneously an antenna at 408 MHz has been interrogated to detect radio emission, if any, in the U.H.F. range. The experiment has been performed at Medicina (25 Km East of Bologna), using the Northern Cross Radiotelescope facilities. A shower striking the scintillator array triggered an oscilloscope on which both 30 and 408 MHz channels were simultaneously displayed. The layout of the scintillator array as well as some details of the recording systems are given in fig.1. The frequency 408 MHz was chosen because, being a radio astronomy band, it is particularly noise free. The purpose of such an experiment was to detect radio emission, if any, at high frequencies, and, in case of positive results, to attempt a frequency spectrum as well as to elucidate if possible the nature of the emission. In this paper technical specifications about the apparatus and the techniques used in building it will be described. Pulses have been seen at 408 MHz as well as at 30 MHz. The analysis of the results and the possible interpretations have been presented elsewhere [14].

1) The Apparatus

Showers were triggered by three plastic scintillators of $\sim 1\ m^2$ of area placed at the vertices of a triangle of 40 m per side. The shower energy was $\gtrsim 5.10^{15}$ eV. Both the 408 MHz and 30 MHz systems were run for a trial of $\sim$1 month with two single three-element Yagi type antenna. Afterward, in order

a) to match the beam of the aerial to the angle of acceptance of the scintillation counters

b) to increase the area of the aerials

c) to increase the gain

new aerials were built: four three element Yagi type antennae at 30 MHz and one 11 Yagi type antenna at 408 MHz.

Fig.1 shows the layout of the two apparatus in the final state. As shown, straight through amplification is used at 30 MHz. The overall bandwidth in both systems is 2 MHz at 3 db down.

2) 30 MHz Antennae

The array was formed of four Yagi type antennae lying at the vertices of a square of side 8.5 m

Table 1 shows the dimensions of one single antenna.

Table 2 shows the characteristics of a single antenna and of the array.

The phasing of the four antennae was obtained by a system of hybrid rings built with 75Ω coaxial cable (Fig.2).

If all terminals of the hybrid ring are loaded and matched, output number three is isolated from number one but not from inputs two and four. Therefore if V_4 and V_2 are two equal input voltages the output

voltage will be:

$$(1) \qquad V_{out} = j \frac{V_4 + V_2}{\sqrt{2}} \qquad (j = \text{imaginary unit})$$

3) Radio Receiver at 30 MHz

3.1- Input Band Pass Filter

It is well known that transistors suffer from cross-modulation and overloading much more than other active devices. In the presently described system, the input transistor stage lacks selectivity being adjusted for low noise operation. Strong out-of-band signals are not efficiently rejected. The band pass filter, by drastically limiting the allowed input frequencies, cuts out all spurious responses. Its insertion loss in equivalent noise temperature loss is negligible compared to the galactic background noise level. In fact the filter attenuation is 2.6 db which means an increase of ~350°K in the receiver temperature.

The diagram of one of the three equal cells used and the values of the components are shown in Fig.3. Fig.4 shows the band of the filter displayed on a Poliskop type SWOB (test set which combines equipment for gain vs. frequency measurements. The frequency range covers 500 KHz to 1200 MHz).

3.2- 30 MHz Pre-Amplifier

In this low-noise high-gain device three germanium transistor stages were used. The input "cascode" circuit was chosen in order to avoid neutralization and also because of its intrinsic

low noise figure.

Fig.5 shows the circuit diagram.

L_2 matches the output impedence of the cascode to the emitter of the following grounded base amplifier. The tuned circuits of the device allow a gaussian-like type of response.

The central frequency is 30 MHz while the band-width is 7 MHz at 3 db down (Fig.6). The power gain is about 36 db.

The input circuit, namely L_1, was adjusted for minimum noise figure, i.e. 1.8 db. This corresponds to a pre-amplifier temperature of $\sim$ 150°K. A high gain stability, necessary in the present experiment, was achieved by the use of AF102 transistors as well as the double highly stabilized DC power supplies, built in the laboratory. No thermal compensations were attempted. Room temperature being kept constant within a few degrees avoided sophisticated devices and protected the rest of the equipment from temperature variations.

3.3- Attenuator

The noise power W of a system can be written:

(2) $$W = \Delta \nu \; K \; T_s$$

where k = Boltzmann constant (1.374×10^{-23} Joule°K^{-1})

T_s = noise temperature of the system in °K

$\Delta\nu$ = band-width in Hertz

At 30 MHz T_s can be considered just the sky temperature (average temperature 2×10^4°K, maximum $4 \div 5 \times 10^4$°K at 30 MHz depending

on sideral time, extrapolated from Ko [15]).

The contribution of the pre-amplifier noise (i.e. 150°K; 500°K with filter) can be neglected. The galactic noise received by the antennae is therefore, rather large. The gain of the pre-amplifier is also large. In such a situation, saturation of the IF amplifier, in series with the pre-amplifier, is likely to occur.

By properly adjusting the attenuator, only a convenient power level is allowed through.

Attenuation can be varied in steps of 0.5 db up to a maximum of 31.5 db total attenuation. Fig.7 shows the circuit diagram; the values of the components are also indicated.

3.4- Amplifier

This amplifier must handle large input signals. For this reason silicon power transistors (2N708) were used.

No problems were found with NF (noise figure). The contribution to total NF after the high gain pre-amplifier is negligible in any case. The amplifier includes four cascaded common base stages with a system of series and parallel tuned circuits. Gain stability is achieved by the use of selected components (i.e. high stability resistors (H.S.R.)) and by highly stabilized DC power supplies as mentioned above.

Regeneration is dealt with by proper stagger tuning and by the common base configuration. The output signal, after this stage, is rather high ($\sim$ 100 mV r.m.s.) and enough for an efficient detection

The gain of the amplifier is about 40 db. The band-width 2 MHz at 3 db down (Fig.8) skirt-selectivity is fairly good and the adjacent channel interference is therefore much reduced. The circuit diagram is shown in fig.9.

3.5- Detector and Delay Line

The radio emission from a shower is a single pulse containing frequency components on a large range of frequencies.
The radiated energy increases as $\nu\Delta\nu$ and the pulse width at the receiver output varies as $\Delta\nu^{-1}$.
The power flux therefore varies as $\nu\Delta\nu^{2}$ while the noise power will vary according to (2)
The signal to noise ratio therefore is given by:
$R \propto \nu\Delta\nu$ for a receiver with a square law detector
$R \propto (\nu\Delta\nu)^{\frac{1}{2}}$ for a receiver with a linear detector
To get a better R a germanium diode detector has been used, which was "square law" up to 300 mV of input and became "linear" for larger signals. The following RF filter was designed keeping in mind the necessity of having a small time constant. The filter was made up of tiny RF choke. The stray capacities compensate for the two missing capacitive "legs" of the Π. The delay line (Columbia HH 1600 cable with magnetic core and 5 MHz bandwidth) allows any radio pulse by EAS to be shown after 6.3 μs on the oscilloscope trace. During the experiment a time base of 1 μs/cm was used.

08 MHz Antenna

or the antenna an 11 elements Yagi type was built. A "balun" matches he coaxial cable (RG8) to the folded dipole and produces the necessay balancing (Fig.10). The length of the "balun" was computed with the

usual formula

(3) $$\frac{\lambda}{2} \cdot \frac{n_a}{n_c}$$

where:

λ = wavelength

n_a = refraction index of the vacuum (~ 1)

n_c = " " of the cable (~ 1.5)

This length in our case turned out to be 240 mm.

The physical dimensions of the 11 element antenna are shown in Tab. 3.

The tubing used was aluminium alloy. The beamwidth was $\sim 30°$ pointed to the Zenith and the gain was $\sim$ 12 db. From

(4) $$A = \frac{\lambda^2 G}{1.64 \times 4\pi}$$ (Kraus [16])

A = area of the antenna

λ = wavelength in meter

G = antenna gain

one obtains $A \sim 5 \times 10^3$ cm^2, a factor $\sim 10^3$ smaller than the 30 MHz antennae system. The bandwidth of the antenna was 20 MHz.

5) Radio Receiver at 408 MHz

At this frequency the galactic noise corresponds to a sky temperature of about 20°K towards the galactic pole and reaches 400°K towards the galactic center [17] , comparable to the equivalent input temperature of a well-made transistor amplifier.

These conditions impose the use of special transistors, well-designed circuitry and careful mechanical housing.
Gain stability and low noise figure, a must at these frequencies, are achieved by carefully choosing components and power supplies.

5.1- Input band-pass filter

An input filter was built mainly because of the two following reasons:

a) to short out the image frequency, namely 348 MHz.

b) to short out strong signals (such as radio links) outside the allowed band in order to reduce cross modulation and saturation effects.

In order to avoid large insertion losses a distributed constant technique has been adopted. The loss was $\sim$ 0.2 db which corresponds to a noise temperature increase of $\sim$15°K.

5.2- R.F. block

The R.F. (radio frequency) includes an R.F. "cascode" amplifier, a diode mixer and an IF preamplifier.
The block itself is built in a single bronze casting unit for best mechanical stability.
The R.F. "cascode" amplifier is made of two low-noise, high-gain germanium transistors. The distributed resonant circuits are housed in proper cavities and adjusted to the proper frequency by micro-trimmers (Fig.11). A band pass output circuit gives the

required frequency response (Fig.12). Coupling to the next stage is obtained by means of an inductive link. Unilateralization was found to be unnecessary.

After the R.F. amplifier, a diode mixer was built made of two series of connected diodes, center-fed by the cascade output link and end-fed by a properly phased R.F. signal from a local oscillator.

The "difference beat" of input (408 MHz) and local oscillator (378 MHz) conveniently filtered, feeds a 30 MHz preamplifier which has been described in sect. 3.2. The gain of the entire block is of the order of 55 db while its noise figure ranges around 3 db at 408 MHz,i.e. a noise temperature of 290°K.

The band-width of the whole block is 8 MHz at 1 db down.

5.3- Local oscillator

In the present experiment the local oscillator used was that of the "Northern Cross Radiotelescope" which operates at 408 MHz.

However, any R.F. oscillator capable of delivering 1 mV in power at 378 MHz would serve the purpose.

From Fig.1 one can see that the following parts of the 408 MHz channel are identical to the corresponding ones of the 30 MHz channel already described above.

5.4- System noise temperature

The temperature of the whole system is equal to the temperature of the antenna plus the receiver temperature.

The whole receiving system has a temperature of 320°K well comparable to the antenna at this frequency.
Under these conditions the signal to noise ratio is always less or at most equal to one, for any detected EAS pulse. Therefore the results had to be analized in a statistical way rather than on a single pulse basis.

Conclusions

With the above described system radio pulses from EAS have been successfully detected during four months of operation [14] . While in preceding experiments at low frequencies the pulse rate was of $\sim$ 1 every 100 showers, in the 10^{15} eV energy range, with the 30 MHz apparatus about 66% of all traces showed a distinguishible pulse above noise. The 30 MHz apparatus, in fact, had a total gain of $\sim$ 75 db at the detector output. This implies that a pulse of 1 cm of height on the scope with sensitivity of 20 mV/cm corresponds to a field strength of $E \sim 1.0\ \mu V\ m^{-1}$. The background noise level during most hours of the day was less than 0.5 cm on the scope trace with the same sensitivity. Therefore with the above described system one is able to detect pulses from EAS whose field stregth is greater than $E \sim 0.6\ \mu V\ m^{-1}$.

Furthermore, the system sensitivity can be estimated from system noise temperature. Having W from (2),one finds from

(5) $$W = \frac{\eta E^2 A}{Z_o}$$ (Kraus, [16])

(η = antenna efficiency = 0.5, Z_o = impedence = 377Ω ,
E = field strength, A = effective area of the antenna)

$$E \sim 0.7\ \mu V\ m^{-1}$$

assuming a minimum sky temperature of 5×10^3 °K. This value of E is well in agreement with the above figure.

The 408 MHz system has a total gain of 105 db, which implies that for a field strength of 0.5 $\mu V\ m^{-1}$ on the antenna one gets a 20 mV deflection on the scope screen. While it is possible, to give an average value of field strength for the 30 MHz pulses; for the 408 MHz radiation, according to the considerations of the sky temperature and the receiver temperature, one can only estimate that the field strength be $E \sim 4.5\ \mu V\ m^{-1}$ detectable above noise. This justifies the fact that the results showed a positive increase at 6.3 μs only in statistical analysis.

With a higher antenna gain one could lower the field limit to acceptable values, but this implies a much narrower antenna beam which, in turn, would lower the EAS counting rate.

Aknowledgements

We are indebted to the Electronic Group of the National Laboratory of Radioastronomy for assistance and advices in building the apparatus.
Mr. S. Cortiglioni and Mr. G.P. Cazzola for running the experiment and Prof. M. Galli for help and criticism are gratefully aknowledged.
Some of the apparatus here mentioned belong to the National Laboratory of Radioastronomy and may have appeared in some other work.

References

ASKARYAN, G.A.
Sov. Phys. J.E.T.P., 14, 441 (1961).

JELLEY, J.V., FRUIN, J.H., PORTER, N.A., SMITH, F.G., WEEKES, T.C., and PORTER, R.A.
Nature, 205, 327 (1965).

KAHN, F.D., and LERCHE, I.
Proc. Roy. Soc. A. 289, 206 (1966).

PRESCOTT, J.R., PALUMBO, G.G.C., GALT, J.A., and COSTAIN, C.H.
Can J. Phys. 46, S246 (1968).

HAZEN, W.E., HENDEL, A.Z., HOWARD SMITH, and SHAH, N.Y.
Phys. Rev. Letters, 22, 35 (1969).

JELLEY, J.V., CHARMAN, W.N., FRUIN, J.H., SMITH, F.G., PORTER, R.A., PORTER, N.A., WEEKES, T.C., MC BREEN, B.
Nuovo Cimento, 46, 649 (1966).

BARKER, P.R., HAZEN, W.E., HENDEL, A.Z.
Phys. Rev. Letters, 18, 51 (1967).

ROSENTHAL, J.L., FILCHENKOV, M.L.
Izv. Akad. Navk., 30, 703 (1966).

CHARMAN, W.N., JELLEY, J.V.
Can. Jour. of Phys., 46, S216 (1968).

FEGAN, D.J., SLEVIN, P.J.
Nature, 217, 440 (1968).

SPENCER, R.E.
Nature, 222, 460 (1969).

CHARMAN, W.N., JELLEY, J.V.
Nuovo Cimento to be published.

CASTAGNOLI, C., SILVESTRO, G., PICCHI, P., VERRI, G.
Nuovo Cimento, 63-B, 373 (1969).

GALLI, M., PALUMBO, G.G.C., SINIGAGLIA, G.
Eleventh Int. Conf. on Cosmic Rays, Budapest to be published.

15 KO, H.C.
Proc. I.R.E., 46, 208 (1958).

16 KRAUS, J.D.
Radio Astronomy, New York, St. Louis, San Francisco, Toronto, London, Sidney, Mc Graw-Hill Company, 1966.

17 HANSEN, R.C.
The Microwave Engineers' Handbook, p. 150, (1965).

Table 1–30 MHz Yagi type 3 element antenna

	Length (mm)	Diameter (mm)
rector	4500	22
›ole	4700	22 and 6
flector	4900	22
stance between elements	1500	
lun length	3300	

Table 2-Characteristics of a single antenna and of the array

Antenna	Beamwidth 3 db down pointed to the Zenith	Bandwidth	Gain	Area
1 Yagi 3 element	70° ± 10°	5 MHz	8 db	4×10^5 cm^2
4 Yagi Square Array	40° ± 5°	2 MHz	14 db	2×10^6 cm^2

Table 3 - 11 elements Yagi 408 MHz antenna

	Length in mm	Diameter in mm
ole	292	12 and 3
ector 1	325	12
2	327	12
3	302	12
4	310	12
5	307	12
6	305	12
7	303	12
8	296	12
9	295	12
lector I		
the director plane	432	12
lector 2 and 3	432	12
mm above and below plane of the directors		
ole and reflector 1		
tance between directors between dipole and reflector 1	180	

Figure Captions

Fig. 1 Layout of the apparatus

Fig. 2 Phasing hybrid ring

Fig. 3 30 MHz band pass filter
Circuit diagram

Fig. 4 30 MHz band pass filter
Bandwidth 4 MHz at 3 db down

Fig. 5 30 MHz Cascode preamplifier
Circuit diagram

Fig. 6 Bandpass 30 MHz cascode pre-amplifier
Bandwidth 7 MHz at 3 db down

Fig. 7 Attenuator circuit diagram

Fig. 8 Bandpass 30 MHz amplifier
Bandwidth 2 MHz at 3 db down

Fig. 9 30 MHz amplifier
Circuit diagram

Fig.10 408 MHz Dipole
Top view

Fig.11 408 MHz R.F. Block
Circuit diagram

Fig.12 Band-pass of the 408 MHz R.F. Block
Bandwidth 7 MHz at 3 db down.

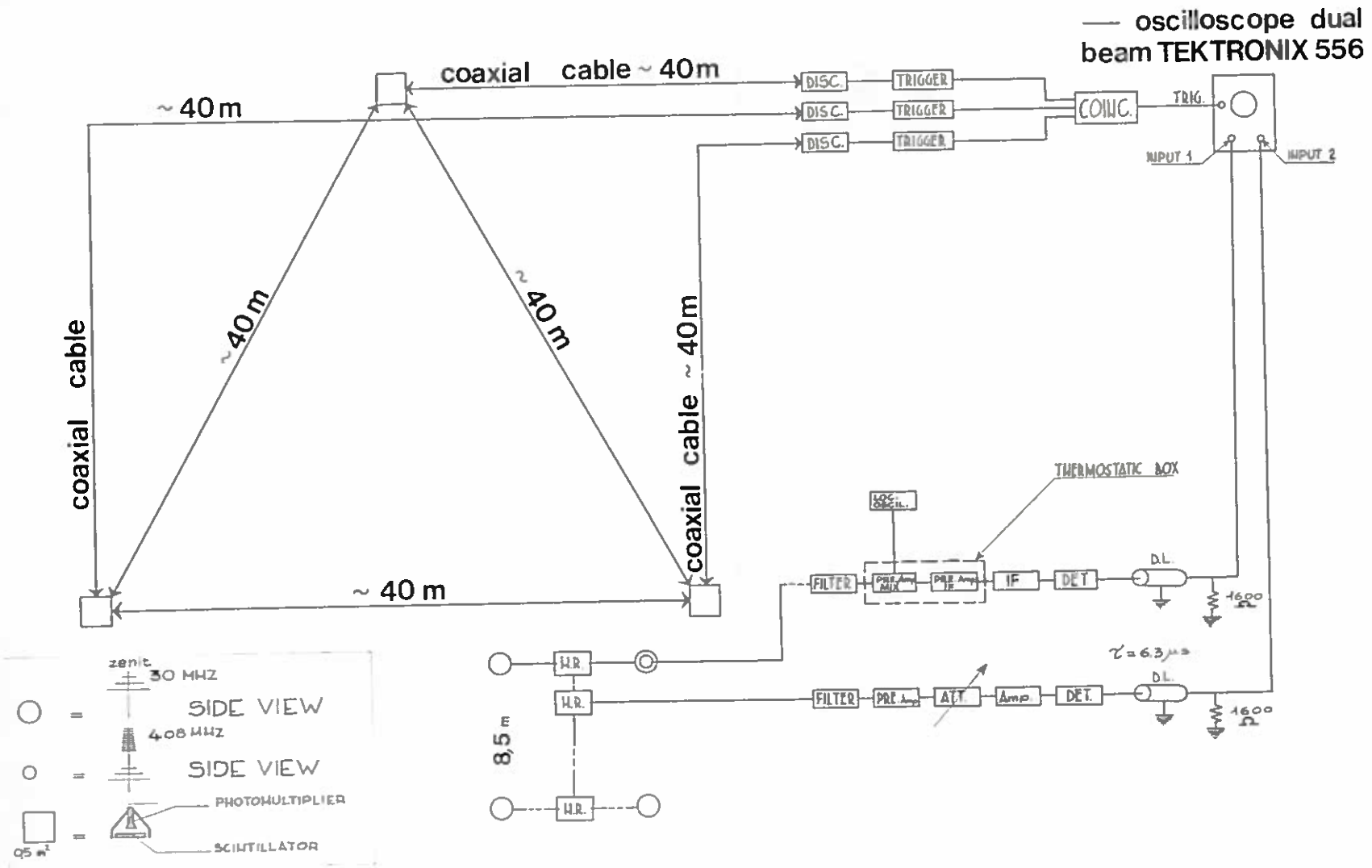
— oscilloscope dual beam TEKTRONIX 556
coaxial cable ~ 40m
~ 40 m
coaxial cable
~ 40 m
~ 40 m
coaxial cable ~ 40 m
~ 40 m
DISC.
DISC.
DISC.
TRIGGER
TRIGGER
TRIGGER
COINC.
TRIG.
INPUT 1
INPUT 2
THERMOSTATIC BOX
LOC. OSCIL.
FILTER
PRE Amp MIX
PRE Amp IF
IF
DET
D.L.
1600 Ω
τ = 6.3 μs
H.R.
H.R.
H.R.
8,5 m
FILTER
PRE Amp
ATT.
Amp
DET.
D.L.
1600 Ω
zenit
30 MHZ
SIDE VIEW
408 MHz
SIDE VIEW
PHOTOMULTIPLIER
SCINTILLATOR
0,5 m²

Fig. 1

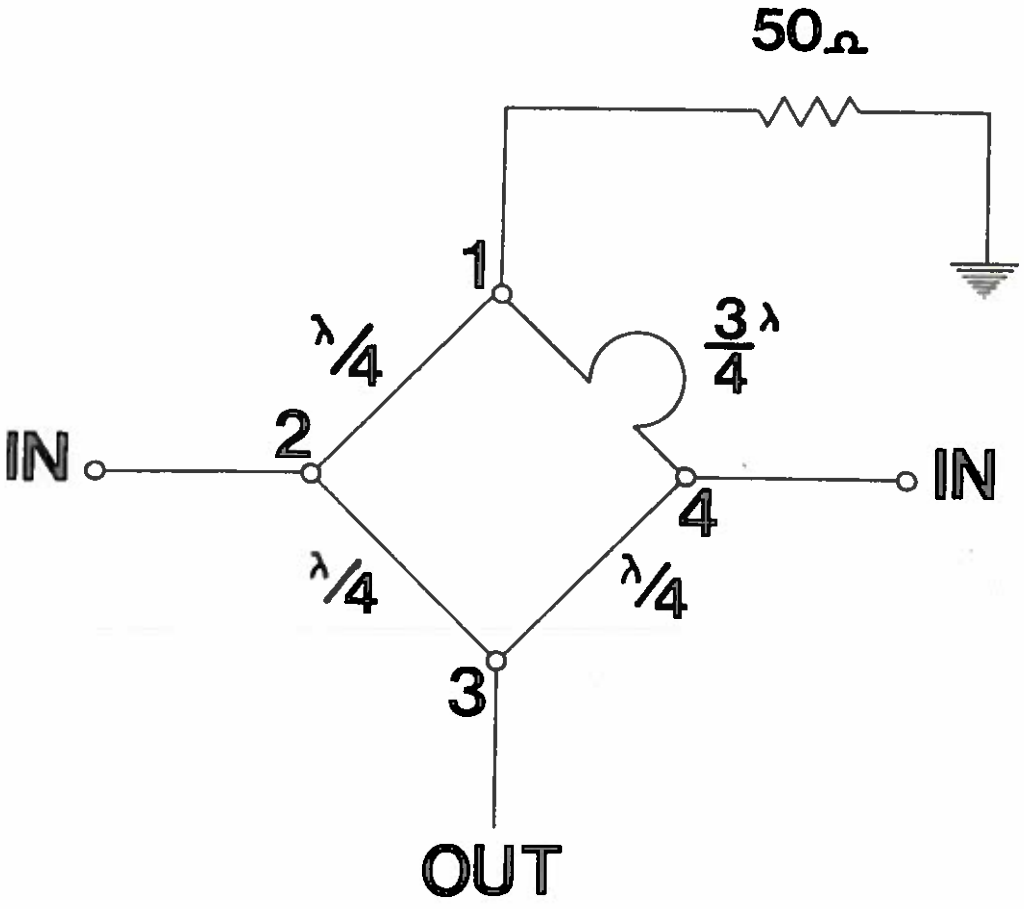

FIG. 2

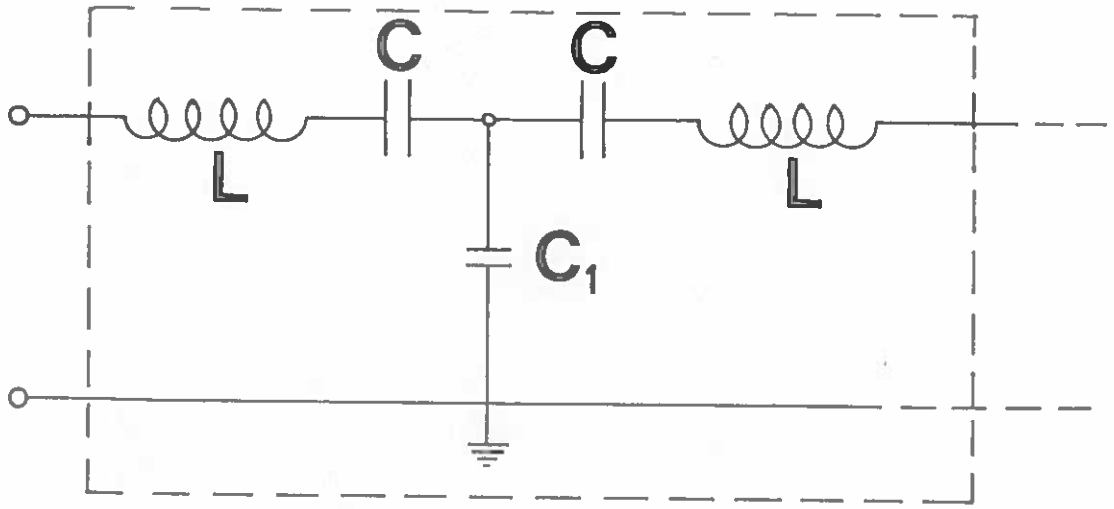

Band = 4 MHZ

L = 2 μH
C = 15 pF
C_1 = 100 pF

FIG. 3

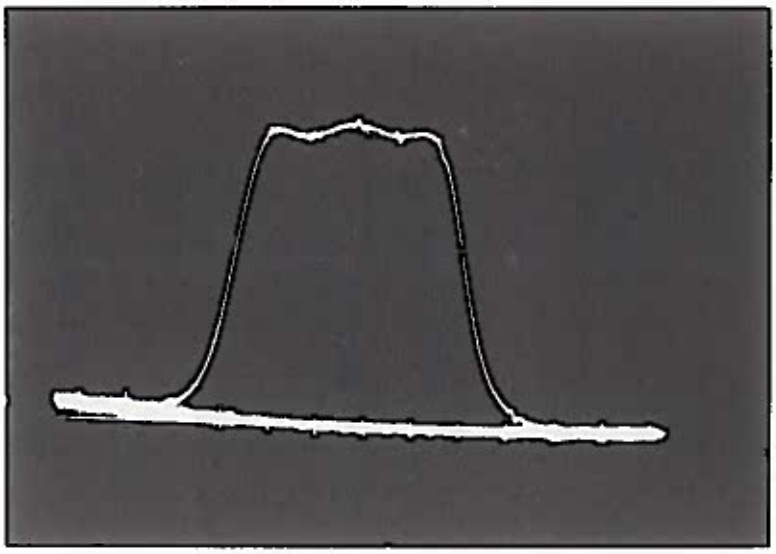

FIG. 4

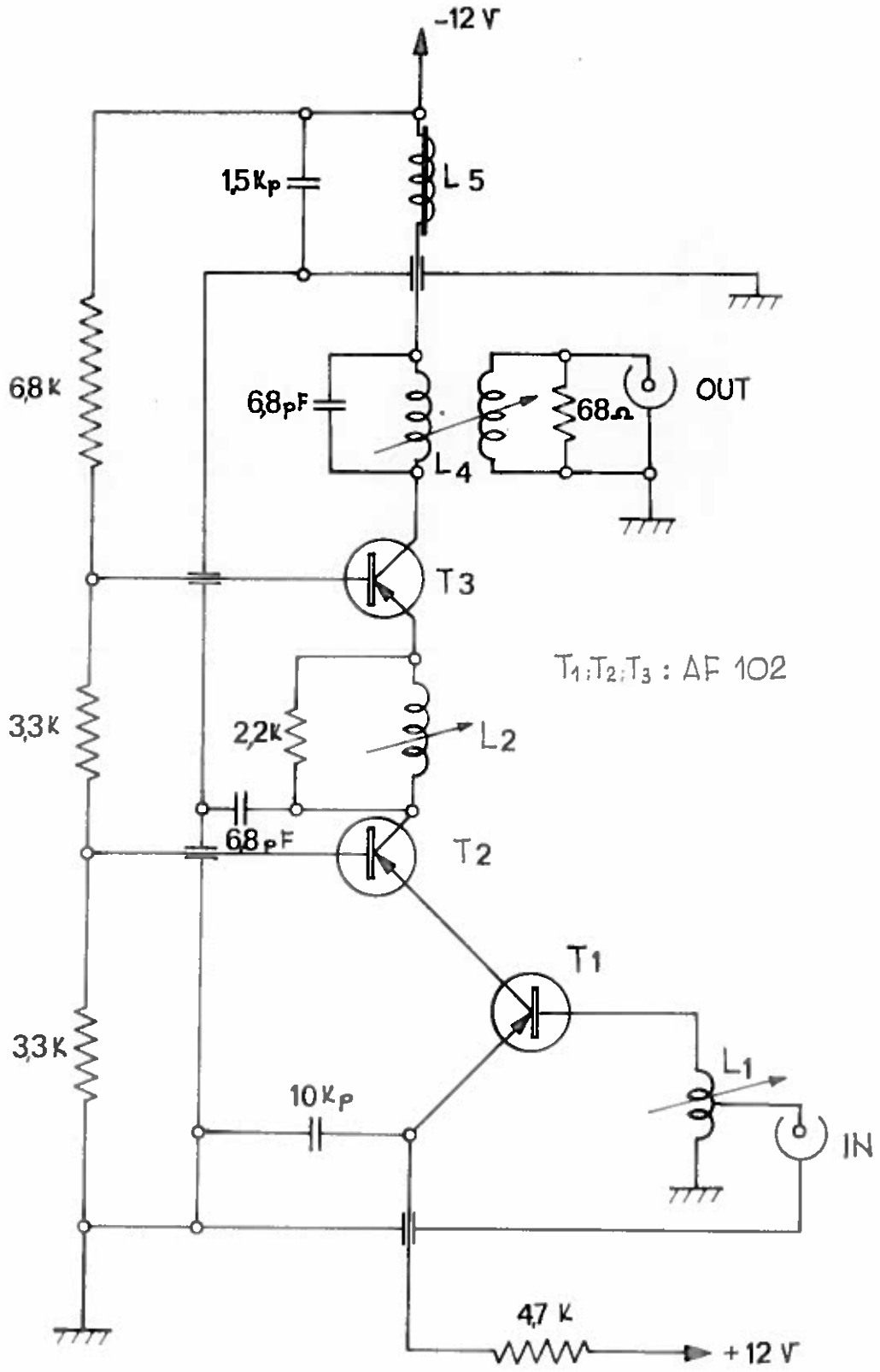
-12 V
1,5 Kp
L 5
6,8 K
6,8 pF
L4
68 Ω
OUT
T3
T1 ; T2 ; T3 : AF 102
3,3 K
2,2 K
L2
6,8 pF
T2
T1
3,3 K
10 Kp
L1
IN
4,7 K
+12 V

FIG. 5

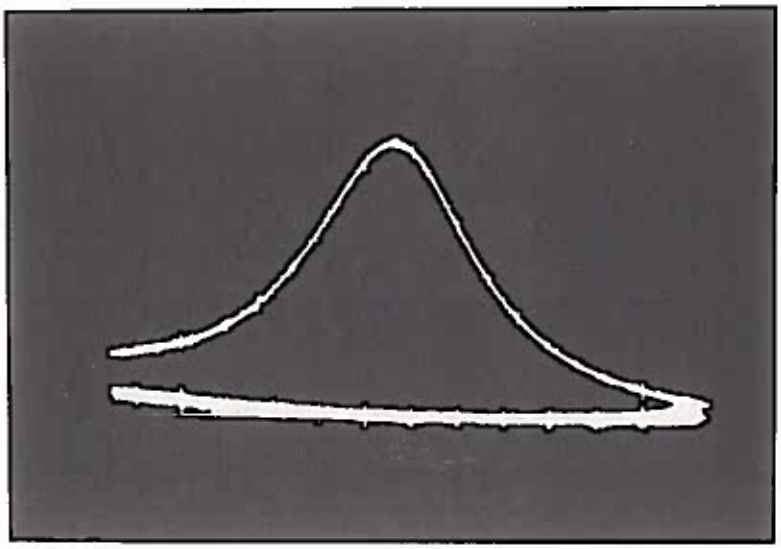

FIG. 6

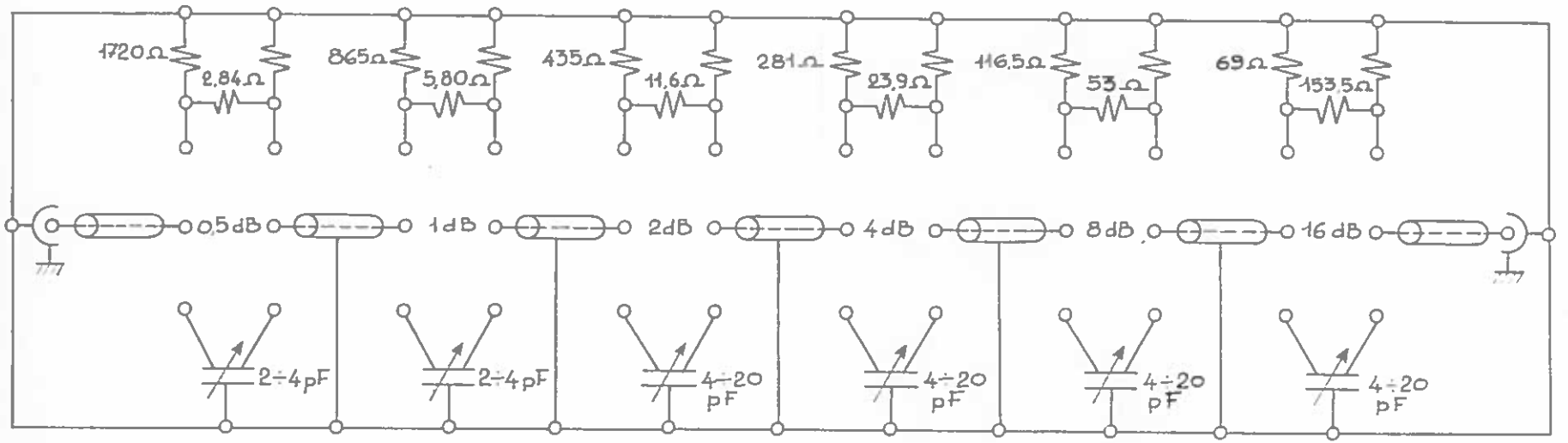
1720Ω
2,84Ω
865Ω
5,80Ω
435Ω
11,6Ω
281Ω
23,9Ω
116,5Ω
53Ω
69Ω
153,5Ω
0,5dB
1dB
2dB
4dB
8dB
16dB
2÷4pF
2÷4pF
4÷20 pF
4÷20 pF
4÷20 pF
4÷20 pF

Fig. 7

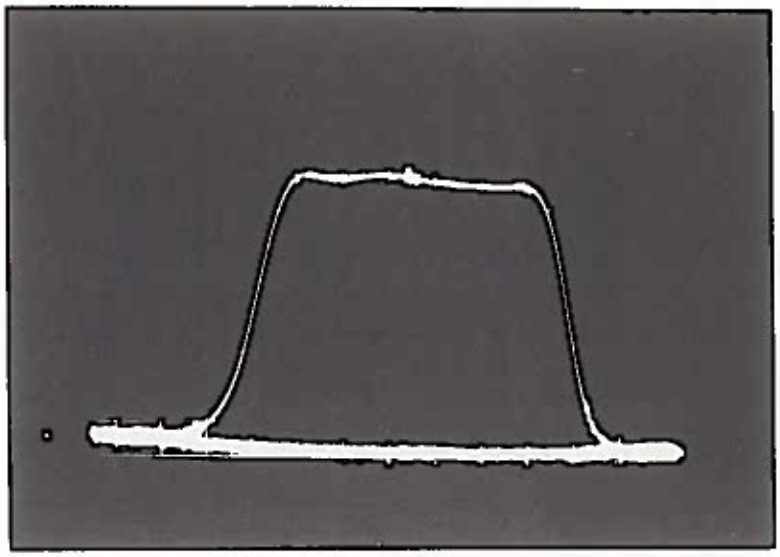

FIG. 8

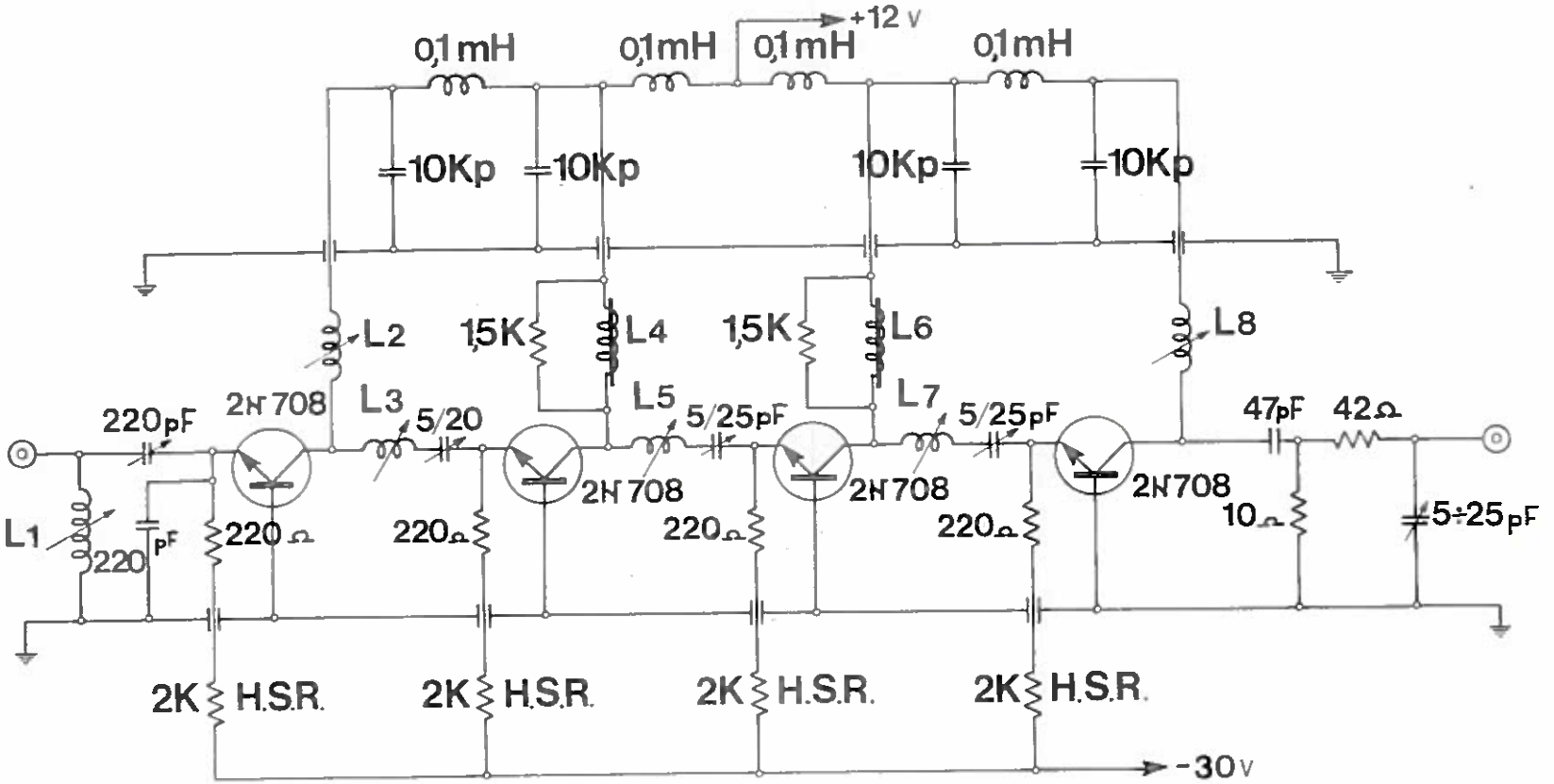

L1 = 0,3 μH TURNS 6 ⌀ 0,3 mm
L2 = 0,5 μH TURNS 8 ⌀ 0,3 mm
L3 = 1,5 μH TURNS 16 ⌀ 0,3 mm
L4 = 0,74 μH TURNS 11 ⌀ 0,8 mm

L5 = 1,3 μH TURNS 13 ⌀ 0,3 mm
L6 = 0,74 μH TURNS 11 ⌀ 0,8 mm
L7 = 0,28 μH TURNS 6 ⌀ 0,3 mm
L8 = 0,53 μH TURNS 8 ⌀ 0,3 mm

Fig. 9

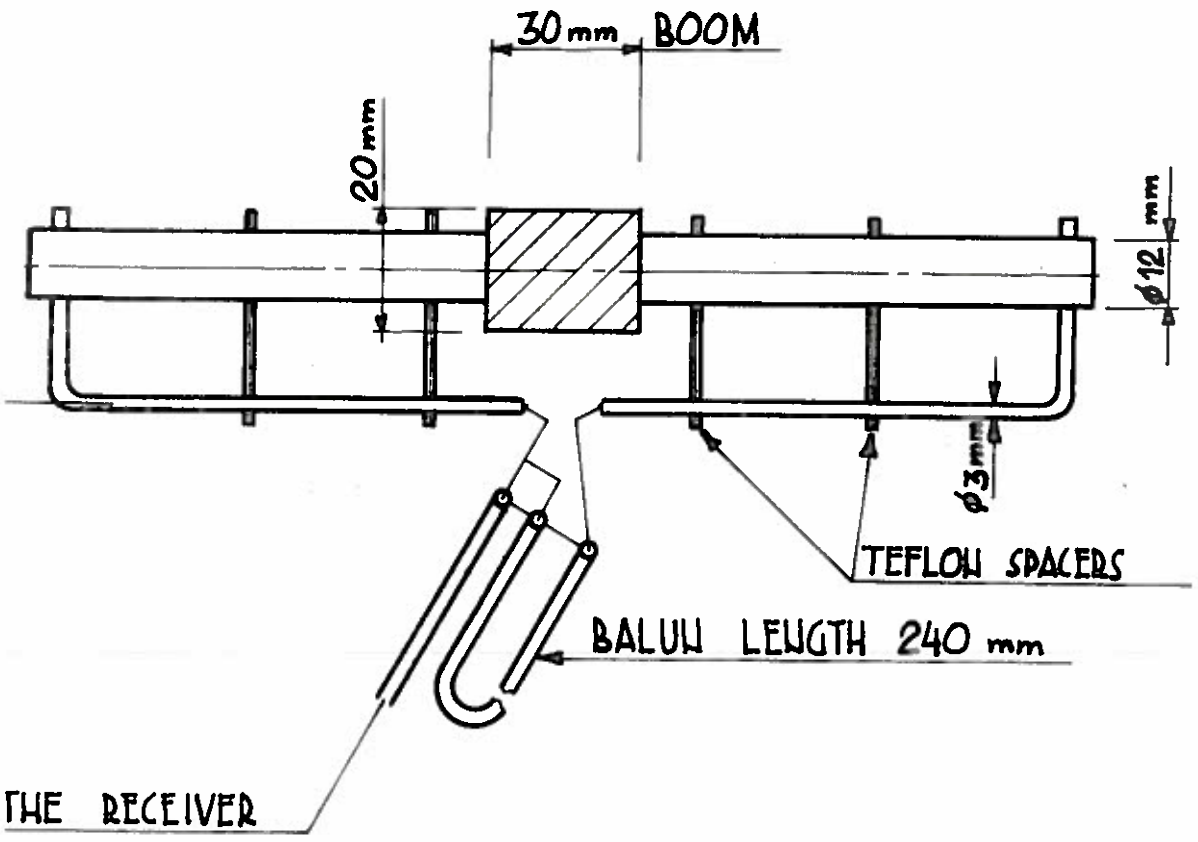
30 mm BOOM
20 mm
φ12 mm
φ3 mm
TEFLON SPACERS
BALUN LENGTH 240 mm
THE RECEIVER

FIG. 10

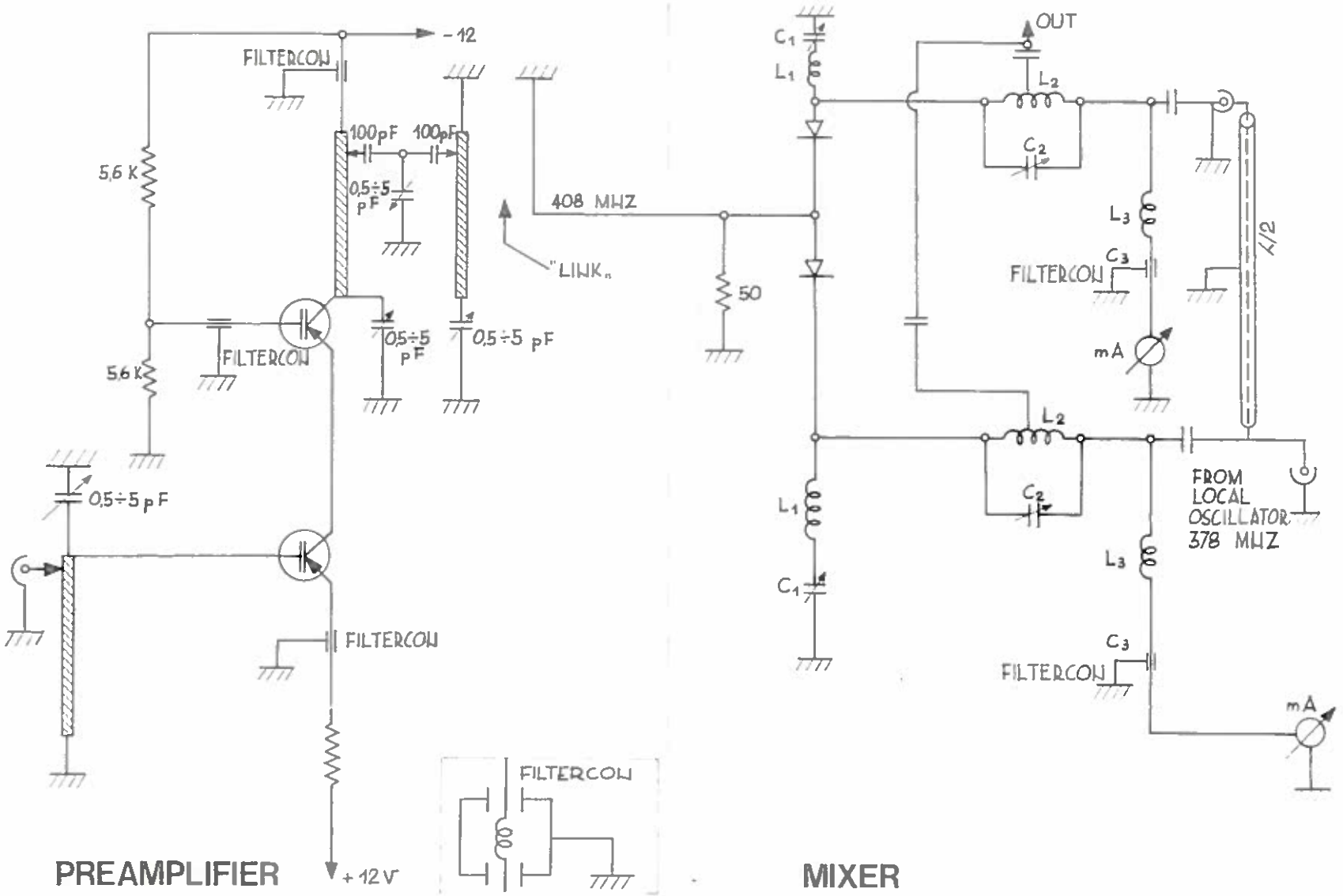
-12
FILTERCON
100pF
100pF
5,6 K
0,5÷5 pF
408 MHZ
"LINK"
50
0,5÷5 pF
0,5÷5 pF
5,6 K
FILTERCON
0,5÷5 pF
FILTERCON
+12 V
PREAMPLIFIER
FILTERCON
C1
L1
OUT
L2
C2
L3
C3
FILTERCON
mA
λ/2
L2
C2
L1
C1
FROM
LOCAL
OSCILLATOR
378 MHZ
L3
C3
FILTERCON
mA
MIXER

Fig. 11

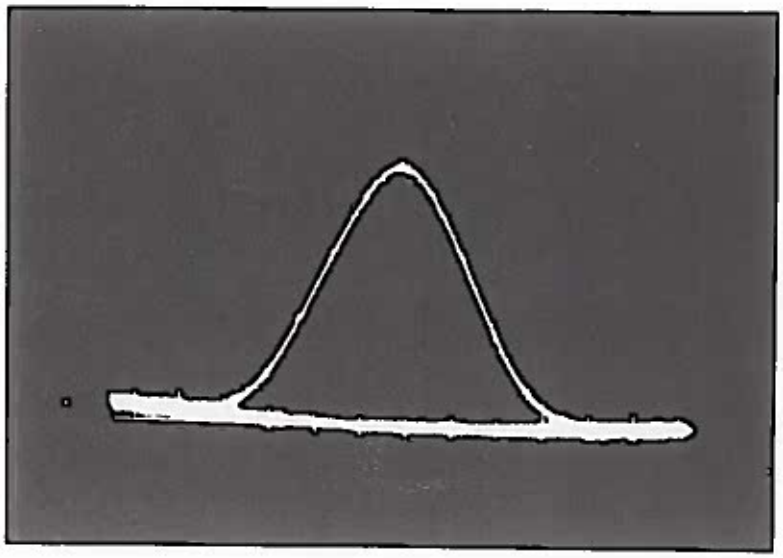

FIG. 12